OPEN ACCESS
Journal of Innovative Optical Health Sciences
2150015 (13 pages)

DOI: 10.1142/S1793545821500152

World Scientific
www.worldscientific.com

Design and validation of a handheld capnography device for cardiopulmonary assessment based on the Arduino platform

Om Prakash Singh*
Bio-signal Processing Research Group (BSPRG)
School of Biosciences and Medical Engineering
Universiti Teknologi Malaysia (UTM)
81310 Skudai, Johor, Malaysia
bioom85@yahoo.com

Ismail M. El-Badawy
Electronics and Communication Engineering Department
Arab Academy for Science and Technology, Cairo, Egypt

School of Electrical Engineering
Universiti Teknologi Malaysia (UTM)
81310 Skudai, Johor, Malaysia
ismailelbadawy@aast.edu

M. B. Malarvili*
Bio-Signal Processing Research Group (BSPRG)
School of Biosciences and Medical Engineering
Universiti Teknologi Malaysia (UTM)
81310 Skudai, Johor, Malaysia
malarvili@biomedical.utm.my

Received 6 February 2021
Accepted 19 April 2021
Published 28 June 2021

The design of a handheld capnography device is in great demand because of its effective and practical uses in all cardiac arrest resuscitations, according to the recommendation of the American Heart Association. Herein, a handheld capnography device that can be used in clinical settings and the home environment is reported. The proposed device was developed by using an infrared CO_2 sensor, Arduino Mega2560, and a high-resolution display (2.8"). Furthermore, two rechargeable batteries (7.6 V, 0.99 A) and a secure digital card with a capacity of 16 GB were incorporated to increase the portability and usability of the device. Algorithms were implemented

*Corresponding authors.

to measure standard features, namely, inspired CO_2 (ICO_2), end-tidal CO_2 ($EtCO_2$), and respiratory rate (RR). The features of 15 healthy subjects were recorded by using the developed prototype and the standard capnography device (Capnostream^{TM}20 Model CS08798). Validation was performed with Bland–Altman plots. Findings revealed that mean differences ± standard deviations for the set limits of ICO_2, $EtCO_2$ and RR were 0.29 ± 1.30 millimeters of mercury (mmHg), 0.15 ± 1.77 mmHg and 0.40 ± 0.97 breaths per minute (bpm), respectively. Most of the differences among device measurements across all features fell within the 95% limits of agreement. Thus, the developed device may help manage respiratory distress conditions in and outside of a hospital setting.

Keywords: Arduino board; capnogram; carbon dioxide sensor; cardiorespiratory; monitoring system.

1. Introduction

The continuous measurement of human respiratory CO_2 by using a capnograph provides valuable information about cardiopulmonary resuscitation, endotracheal tube placement, pulmonary embolism, and procedural sedation, as well as information about the effect of air pollution on cardiopulmonary characteristics and the effectiveness of a treatment for a patient with respiratory distress (specifically asthma, chronic obstructive lung diseases, and congestive heart failure).[1–7] Existing CO_2 measurement devices, such as arterial blood gas, arterialized capillary blood gas, and venous blood gas analysis devices, are considered to be the gold standard in clinical practice.[8–10] However, these devices are invasive, require the recurrent collection of blood samples for CO_2 measurement, and possess several limitations; for example, their use requires expertise and skills; they cause pain to the patient and blood loss; and they involve time-consuming processes that pose hazards and inflict damage to tissue, nerves, and vessels.[11,12] Moreover, they measure only the current respiratory rate, which may change drastically within a short period.[13] These demerits may be overcome by the use of a noninvasive and continuous CO_2 measurement device, such as a capnograph. A study conducted by Transparency Market Research revealed that the need of the global market for capnography devices is about to grow by US $0.6156 billion by the year 2020 due to the increasing incidence of respiratory diseases that require effective treatment.[14] However, the currently available capnograph device is bulky and expensive.[15,16] Hence, a strong need exists for an inexpensive and light-weight device that is similar to a capnograph and that can be used in clinical settings and the home environment to manage respiratory distress by measuring a minimal set of parameters, such as inspired CO_2 (ICO_2), end-tidal CO_2 ($EtCO_2$), and respiratory rate (RR).

Over the past several years, few attempts have been made to develop time-based capnography by using diverting and nondiverting techniques. In 2013, Santoso and Dalu Setiaji[17] presented a diverting capnograph that uses a nondispersive infrared (NDIR) CO_2 sensor, ATmega8535, and display modules (an organic light-emitting diode [LED] seven-segment display with a resolution of 128×64) to measure $EtCO_2$, RR, and CO_2 signals. Nevertheless, the limited data memory, program memory, and universal asynchronous receiver/transmitter (UART) of the microcontroller restricts sketch length and communication mode. In addition, the use of two displays increases the complexity of the system and the computation cost of the device.[17] Subsequently, Bautista *et al.*, developed an alternative capnograph that uses a sprint infrared (IR) sensor, a microcontroller (ATmega328), a LED display, and a Bluetooth module. However, the device can only display CO_2 concentration values.[18] Zaharudin *et al.*, reported a respiratory CO_2 measurement system for home monitoring that uses the MG-811 CO_2 sensor.[19] However, the device was tested only on five subjects. Hence, the used sensor has insufficient efficiency in detecting human respiratory CO_2.[19] Sameen *et al.*, reported a portable respiratory CO_2 monitoring device that is based on the nondiverting technique.[20] In this device, the inconsistency of the capnogram curve complicates quantifying other essential features from the shape of the CO_2 signal.[20] Additionally, the sampling rate (20 Hz) of the used sensor is insufficient for processing the obtained

CO_2 signals; thus, resampling is required and may increase the computation cost of the device. Between the technologies used to develop capnography devices, the diverting technique is considered because it is more convenient, easier to use, and more widely available than nondiverting technology in clinical and hospital settings.[21] Moreover, it enables capnography monitoring even when a patient is in an unusual position.[17] Hence, in this work, we proposed to develop a handheld and light-weight capnography device based on the diverting method that could be utilized in clinical settings and the home environment.

The complete research flow of this study is presented as follows. A block diagram is presented in Sec. 2.1 to provide an overview of the proposed device. The computation and transmission processes and processing algorithm which includes noise reduction, feature computation, and transmission algorithm, of the proposed device are described in Sec. 2.2. The data collection and recording procedures used to determine the performance of the developed device are explained in Sec. 3. The obtained results are presented in Sec. 4, and the findings are discussed in Sec. 5. Finally, the conclusion and the future direction of this research are provided in Sec. 6.

2. Methodology

2.1. *Block diagram of the proposed capnography device*

The block diagram of the proposed capnography device is depicted in Fig. 1. The device consists of four main parts: a CO_2 acquisition unit, processing unit, real-time control (RTC) unit, and display unit. The CO_2 signal is attained from the subjects through a sampling tube and then diverted to the microcontroller unit for the purpose of computation and transmission. A high-resolution display is used to display the CO_2 signal and other parameters, such as maximum and minimum CO_2 concentrations, breathing rate, and activity through serial communication. The RTC unit performs the data logging into a secure digital (SD) card which is being controlled by the processing unit. Each of these parts is explained in detail in the following sections. In addition, a schematic, breadboard and printed circuit board (PCB) layout of the proposed device are illustrated in supplementary Figs. S1–S3, respectively.

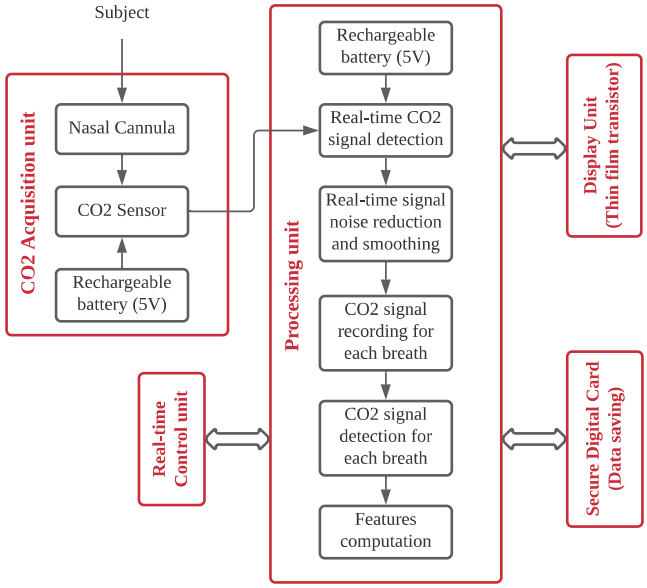

Fig. 1. The overall block diagram of the proposed prototype capnography device; the CO_2 acquisition unit consists of a nasal cannula, water trap, pump, motor, and CO_2 sensor, the processing unit (ATmega2560) elucidates the data transmission and computation, the display unit (2.8", TFT) displays the CO_2 signal, ICO_2, $EtCO_2$, and RR via SPI, the RTC unit provides an accurate timing, and the features are saved into a SD card.

2.1.1. *CO_2 acquisition unit*

The CO_2 acquisition unit consists of five main components: a sampling tube, direct current (DC) motor, pump, moisture trapper and CO_2 sensor. A nasal cannula, with a length of seven feet, is placed between the water trap and subject to transport the CO_2 samples. The incorporated water trap is highly sensitive and traps the moisture and patient secretions while maintaining the morphology of the CO_2 signal. In addition, a $0.2\,\mu$ hydrophobic porous and particular ($200\,\mu$) filters were integrated with the water trap to eliminate the residual water vapor from gas samples while keeping a laminar flow which minimizes the distortion of the CO_2 waveform. The aforementioned features introduced solutions to problems that have previously posed challenges to the capnograph in the intensive care unit (ICU), intensive cardiac care unit (ICCU), neonatal intensive care unit (NICU), critical care unit (CCU), and

intra-transport applications. Thereafter, the CO_2 samples were drawn from the nasal cannula until the speed of the CO_2 sensor reaches 50 milliliters per minute (ml/min) by using the pump and DC motor that allow using the proposed device at a high RR of 150 breaths per minute (bpm). Furthermore, the CO_2 samples were drawn at a sampling rate of 100 Hz via the IR CO_2 sensor, which has a response time of 2 s. The sensor has 3-pin UART communication at the transistor–transistor logic (TTL) level for transmitting and receiving the CO_2 data between the sensor and the microcontroller.

2.1.2. *Processing unit*

The Arduino mega 2560 is employed to process the CO_2 samples for computation and transmission purposes. The Arduino is an open-source microcontroller board that is based on the ATmega2560. It is used in UARTs fashion to read TTL (5V) inputs from external switches, buttons, displays, sensors, etc. It contains a 16 MHz crystal oscillator, power jack, universal serial bus (USB) connection, in-circuit serial programming (ICSP) header, and reset button. The reset button is required for driving the microcontroller by connecting a USB cable to a computer or power supply with an alternating current (AC) to DC adapter or battery. Also, the Arduino board can operate on an external power supply of 6 V to 20 V. However, the recommended power supply range is 7 V to 12 V. Besides, it displays the CO_2 data from the CO_2 sensor on the serial port simultaneously, which is not possible for Arduino Uno with higher baud rates of 19,200 and 115,200 bits per second (bps).

The Arduino integrated development environment (Arduino IDE) software is used to program the Arduino Mega 2560 based on the processing IDE which is installed in the computer. It uses a simple C-based code (other programming languages, such as Splish, can also be used) to operate the Arduino that is known as a sketch. A collection of sketches for a specific purpose is referred to as a library which often makes the programming task simpler for the programmer as the code is hidden inside the library. The computation and transmission algorithms were implemented on an Arduino sketch by using the necessary libraries in addition to local and global variables.

2.1.3. *Real-time control (RTC) unit*

The RTC module (DS3231) is used to save the recorded data on the SD card with the respective date and time to follow up the information of the subjects. The module is composed of a low-cost and extremely accurate inter-integrated circuit (I2C) real-time clock in addition to an integrated temperature-compensated crystal oscillator. It is incorporated into a 3 V lithium battery to maintain an accurate timing when the main power supply of the device is interrupted. The RTC unit maintains seconds, minutes, hours, day, date, month, and year information. Moreover, it automatically adjusts months with a fewer number of days than 31, including alteration of the leap year. In addition, it is easy to be integrated with a microcontroller.

2.1.4. *Display unit*

The Adafruit thin film transistor (TFT) is used for displaying the CO_2 signal and its associated features. The display is large (2.8" diagonal), bright (four white-LED backlight), colorful, and has a four-wire resistive touchscreen. It can be drived with a minimum power supply of 3 V. Additionally, it has a higher resolution of 240×320 pixels than an organic LED that has a resolution of 128×64 pixels. Also, it has a built-in controller with a random access memory (RAM) buffer which reduces the work of controlling. The display can be interfaced with the microcontroller in two modes: 8-bit or serial peripheral interface (SPI). For an 8-bit interface, there is a need of 8 digital data lines and 4 or 5 control digital lines to read and write to the display, whereas the SPI mode requires only 5 pins: SPI data in, data out, clock, select, and d/c. However, an 8-bit mode has a higher transmission speed of data compared to the SPI. On the other hand, the SPI mode is preferable over the 8-bit mode when the speed of data does not mandate. In addition, the SPI mode is simple, fairly flexible, and easily interfaced with various microcontrollers. It also allows the use of micro SD card on the same SPI bus, which is not supported in an 8-bit mode. Therefore, this display module (TFT-2.8") is employed in this work to develop a small and user-friendly CO_2 measurement device. The following section discusses the algorithms that are used for the processing of the CO_2 signal.

2.2. *Noise reduction, feature computation and transmission algorithms*

2.2.1. *Noise reduction algorithm*

Low-pass filter: A first-order finite impulse response (FIR) low-pass filter (LPF) is implemented in the Arduino IDE to restrict the bandwidth and increase the sharpness of the CO_2 signal. The cut-off frequency (f_c) of the filter is set to 10 Hz[22] with a sampling time of 0.01 s. The filter's transfer function is given by Eq. (1).

$$H(S) = \frac{\omega_c}{S + \omega_c}. \tag{1}$$

Where $\omega_c = 2\pi f_c$.

Moving average filter: A moving average filter (MAF) is included in the Arduino IDE to provide a smooth CO_2 waveform, by removing high frequency components,[23] and consequently reduce the overall computation cost of the device. The filter's span width is set to eight based on the trial and error method[24] that analyzed a set of datum points by creating a series of averages of different subsets of the full data sets. This filtering process is implemented by using Eq. (2).

$$y(n) = \frac{[y(n+m) + y(n+m-1) \cdots + y(n-m)]}{2n+1}. \tag{2}$$

Where $y(n)$ represents the average value of n-points, m indicates the neighboring data points on either side of $y(n)$, and $2n+1$ is the span width.

2.2.2. *Features computation algorithm*

Figure 2 shows the flowchart for the algorithm that is used to acquire the CO_2 signal and compute its features (i.e., ICO_2, $EtCO_2$, and RR). The UART mode is initialized; baud rate - 19,200 bps, data - 8 bits, stop bit - 1 bit, and parity - none and the local and global variables are defined in the Arduino IDE. The UART send (T_x) and receive (R_x) pins of the CO_2 sensor are connected to the serial port of the microcontroller to transmit and receive CO_2 data from the sensor to the microcontroller and vice-versa. Thereafter, the sensor is activated and 100 data packets are obtained every second (i.e., the sampling rate is 100 Hz).

The CO_2 data is available with each data packet while ICO_2, $EtCO_2$, and RR are accompanied with last three data packets along with the CO_2 data. Besides, Test_Log Macro is incorporated into the Arduino IDE to verify the data packet reception and other text information during the debugging process. Furthermore, a new baud rate of 115,200 bps is assigned to visualize the data on the serial port of the computer. Both baud rates 19,200 and 115,200 bps are defined as Serial and Serial 1, respectively. Serial and Serial 1 indicate the transmission speeds of the data packets received from the CO_2 sensor and transmitted on the serial port of the computer, respectively.

Serial 1 finds out the data packets with 0×80 and stored into the buffer with index zero by clearing and resetting the buffer. Subsequently, it prints the new data packet on a new line on the serial port, displays and logs the same data on the serial terminal via Macro. The next data packet illustrates the length of a data packet and provides the data information. If the second data packet is 0×04, then it accompanied only CO_2 data (CO_2WB1 and CO_2WB2) and the state is known as without deep packet inspection (DPI). If the second data is 0×07, then it consists of CO_2, ICO_2, $EtCO_2$, and RR and this condition is known as with DPI. Furthermore, the received data packets are cross-checked with the checksum byte and stored into the buffer with an increment of one to the index. The checksum is calculated by using Eq. (3).

$$\begin{aligned}\text{Checksum} = (&\sim (\text{Sum of all bytes in packet} \\ &\text{including start of byte in Hex}) + 1) \\ &\& \ 0 \times 7\text{F}\end{aligned} \tag{3}$$

If the checksum and last data packet are the same, then the rest of data packets are computed. Otherwise, the data is thrown away and the packet is rearranged into the buffer and look for the new data packet. The authenticated data (CO_2, ICO_2, $EtCO_2$, and RR) are then calculated as follows:

$$\text{CO}_2 = \frac{(128 \times C1 + C2) - 1000}{100}, \tag{4}$$

$$\text{ICO}_2 = \frac{128 \times I1 + I2}{10}, \tag{5}$$

$$\text{EtCO}_2 = \frac{128 \times P1 + P2}{10}, \tag{6}$$

$$\text{RR} = \frac{128 \times R1 + R2}{10}. \tag{7}$$

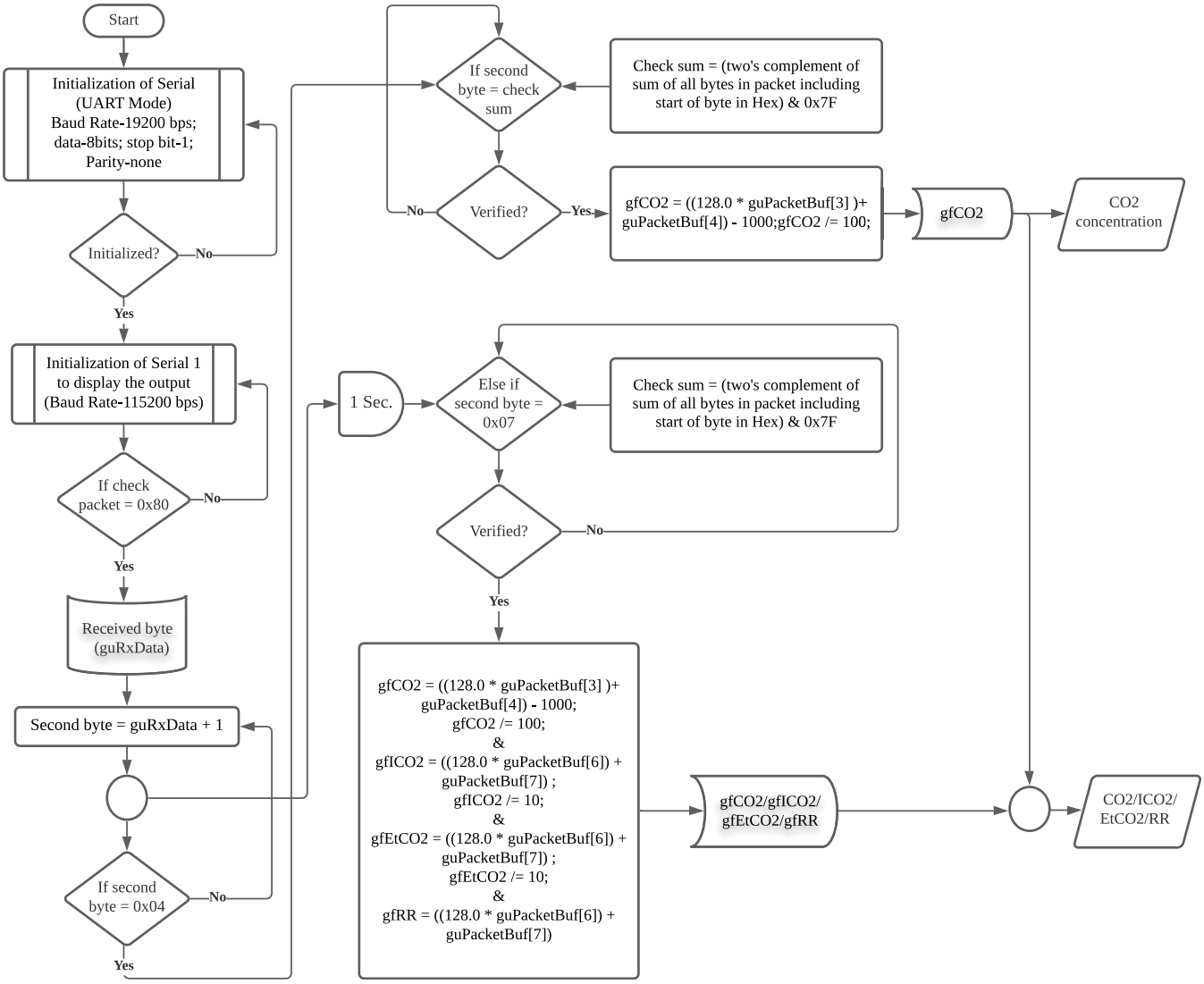

Fig. 2. Flowchart for features computation (the algorithm is programmed and implemented using the Arduino IDE).

Where, $C1$, $C2$, $P1$, $P2$, $R1$, R2, $I1$, and $I2$ are analog data packets which are received from the CO_2 sensor with and without DPI.

2.2.3. *Features transmission and display algorithm*

The flowchart presented in Fig. 3 shows the algorithm that is employed for transmitting and displaying the CO_2 waveform and its features onto the display. Initially, local and global variables in addition to necessary hidden libraries, such as SPI.h, Adafruit_GFX.h, and Adafruit_HX8357.h are defined in the Arduino IDE for SPI and TFT by enclosing the IM2 jumper. Next, the output pins (CS, DC, RST, CLK, MISO, and MOSI) of the TFT are connected to pin numbers 52, 50, 51, 10 and 9 of the microcontroller, respectively, to set up the communication between the host and display. Furthermore, an analog pin is attached to increase the background brightness of the TFT which is activated by providing a power supply of 5 V from the Arduino board. Meanwhile, a communication link is established between the CO_2 sensor and host and vice versa to retrieve the CO_2 data and its features.

A rectangle is prepared with a length and width of 435 mm and 290 mm, respectively, to display the CO_2 signal. In this, length and width denote horizontal and vertical axes, respectively. The horizontal axis represents the time with a span of 0–20 s with 5-s intervals, while the vertical axis represents

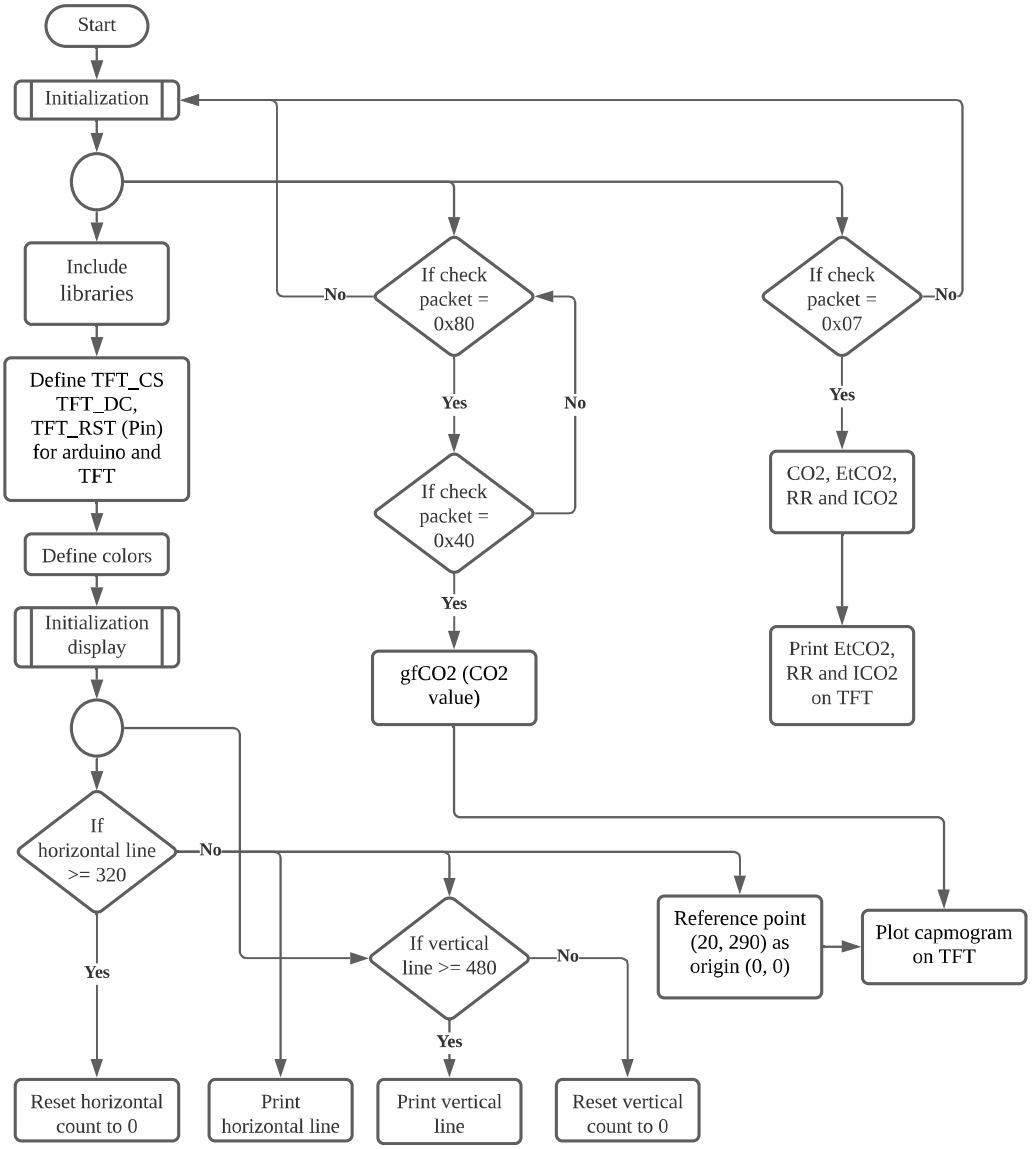

Fig. 3. Flowchart for features transmission and display (the algorithm is implemented in the Arduino IDE by using the Arduino C language).

the exhaled CO_2 concentration in millimeters of mercury (mmHg). The upper and lower limits of the vertical axis are kept between 0 mmHg and 80 mmHg, respectively, with 40 mmHg difference. The difference is printed on the display.

To start the plot of the CO_2 signal, a reference point (20, 290) is selected which is located towards the left-hand side of the rectangle. The CO_2 signal is printed above the reference point to provide a proper visualization of the waveform. The built-in real-time clock of the controller is used for time configuration of the CO_2 signal display. For this, a Boolean variable (display 1) is defined to store the time from the RTC whenever the time exceeds 20 s. The text size, background color of text, starting cursor point, and size of feature values are defined with integer values (0–5).

Lastly, the extracted features along with the CO_2 signal are displayed on the TFT by using the TFT display function (Adafruit_HX8357 TFT = Adafruit_HX8357 (TFT_CS, TFT_DC)). This function requires the TFT structure, coordinates of the starting point, features to be displayed, text color, and lengths of the axes. Thus, the extracted features and CO_2 values are included into the TFT function for the purpose of printing all the values onto the display unit. Hence, the TFT function is called on receiving each valid data packet of CO_2, ICO_2,

Fig. 4. Illustration of the subject's position during the CO_2 signal recording via nasal cannula with a length of seven feet. (a) female, age: 21 and (b) male, age: 28.

$EtCO_2$, and RR. Therefore, whenever a valid data packet is received from the host, the CO_2 concentration, and associated features are calculated and printed onto the display unit through SPI. The following section presents the data collection protocol that is used in this study.

3. Data Collection and Analysis

The subjects are instructed to sit idly on a chair without any physical movement to avoid the change in the CO_2 signal and incorporated features during the recording. Thereafter, each subject is asked to breathe in and out comfortably after placing the sampling tube nearby his/her nose and inserting prongs into it, as shown in Fig. 4, to avoid the alternation in the reading. The CO_2 data recording is conducted on 15 subjects, for 2 min each, using the standard capnography (Capnostream^{TM}20 Model CS08798) and proposed device as advocated by Zhang *et al.*,[25] for further signal analysis. The sampling frequency (f_s) of the existing standard capnography is 20 Hz, while that of the proposed device is 100 Hz; hence offer a freedom for detailed data analysis. The accuracy of the proposed device is validated by using the Bland–Altman's plot (drawn using MATLAB R2015a, Version 8.5) with $p < 0.05$ and limits of agreement set to ±10%–20% of the actual CO_2, $EtCO_2$, and RR values, respectively.[26] The results are presented and discussed in the subsequent sections.

4. Results

Figure 5 shows the internal arrangement of electronic components that are used in the proposed handheld capnography device. These components are placed on a double-sided PCB which is designed for the proposed prototype. The bottom layer of the PCB carries the CO_2 sensor, pump, and DC motor, while the upper layer accommodates the microcontroller and RTC unit. The display is fitted on the top of the board as shown in Fig. 5. A rechargeable battery of 7.4 V and 0.99 A is used to provide a constant supply of 5 V via the voltage regulator IC 7805. Two simple mechanical switches are used to deliver the constant power supply to the sensor and microcontroller. Additionally, a third switch is placed in the SD card slot of the display to control the recording and saving of CO_2 data and its features into the SD card. Moreover, this third switch

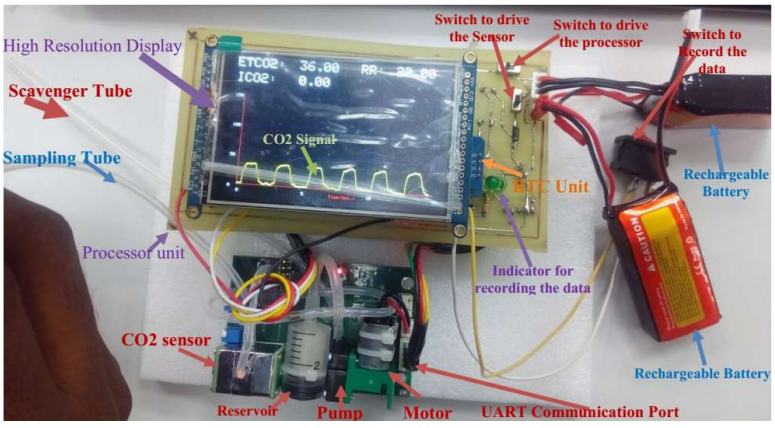

Fig. 5. Internal arrangement of the used electronic components, placed on the PCB of the final model.

controls the LED that is placed at the top of the board, beside the display (see Fig. 5). This LED serves as an indicator for the data recording and therefore helps to identify the fault in the SD card. That is, the SD card is in a need to be formatted if the switch is pressed and the LED is still off, otherwise (i.e., if the LED is turned on when switch is pressed) the recording is in progress. This facility makes the device simpler, user operable and friendly.

The complete device prototype is integrated into two levels through a divider holder with a size of $0.4 \times 0.2 \times 0.2$ inches that is above the first level by 1.2 inches. The CO_2 acquisition unit including the sensor, pump, DC motor, and rechargeable battery is placed in the first level, whereas the processing and RTC units are placed at the divider ($4.6 \times 2.4 \times 0.4$ inches) in the second level. Both levels are placed inside a case with a size of $4.5 \times 3.1 \times 1.8$ inches and wrapped with a top cover that is designed and printed by using SolidWorks and 3D printer, respectively. Hence, the weight of the device is reduced to be less than 450 g.

The design specifications of the top cover, display slot, LED, and third switch are $4.6 \times 4.8 \times 0.4$ inches, 3.6×2.22 inches, 0.24 inches (diameter), and 0.8×0.56 inches, respectively. All the components are mounted next to each other on the top cover of the box to provide a suitable access to the user interface (Ref. video S3). A water trap integrated with a Nafion^{TM} tube is used to retrieve the CO_2 samples from users via a sampling tube. Both items (i.e., water trap and Nafion^{TM} tube) are placed outside the case to provide the option of disposing and replacing them simply by the users which accordingly increases the ease of use of the device.

Figure 6 shows the display of the proposed device, during recording, in idle and active modes. In the idle mode (when the cannula is not attached to a subject), the CO_2 signal and extracted features are shown as null (see Fig. 6(a)). In the active mode (when the cannula is attached to a subject), the CO_2 waveform and its associated features are displayed (see Fig. 6(b)). Figures 7(a) and 7(b) show sample capnogram signals (i.e., CO_2 signals) which are recorded using the proposed and standard capnography devices, respectively. In our work, the recorded CO_2 signal is smoothed by employing a real-time filtering algorithm, as described in Sec. 2.2, that is integrated with the device.

The proposed device is tested and validated in two ways to verify its performance. First, a technical test is carried out to ensure that there are no momentous issues (mainly associated with the user-friendly operability) regarding the basic operation of the prototype. This test confirmed that switches and LED are quite responsive and the display is decently clear. Second, a relative verification is performed to investigate the consistency between measurements of the proposed prototype and those of the standard capnography (Capnostream^{TM}20 Model CS08798) by using the Bland–Altman plot.

4.1. *Performance evaluation*

In this study, 6 male and 9 female healthy subjects aged between 20 and 35 were recruited according to the random sampling method.[26] Table 1 lists the demographic details of these subjects. A written informed consent form was collected from all the subjects with no history of smoking, recent upper respiratory infection, fever, and significant cardiopulmonary or noncardiopulmonary disease before being involved in the study. In addition, descriptive statistics were estimated for all the subjects. For males and females, Shapiro–Wilk p- and z-values were calculated to verify the normality of each

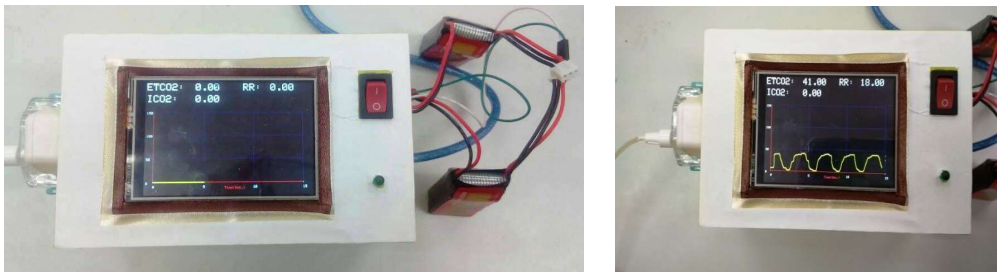

(a) (b)

Fig. 6. The proposed device's display in (a) idle and (b) active modes.

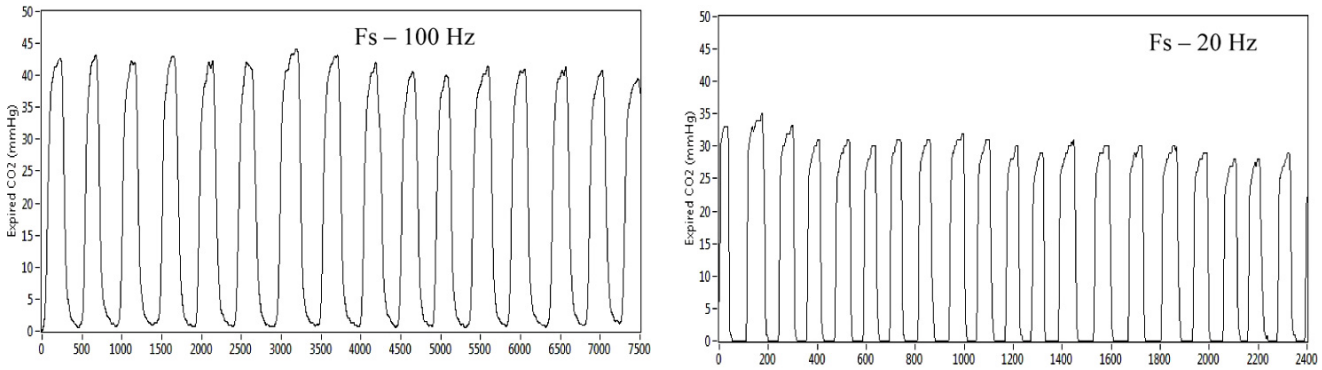

(a) (b)

Fig. 7. Sample recorded CO_2 signals using the (a) proposed device and (b) standard capnography device (Capnostream^{TM}20 Model CS08798), with a sampling frequency (f_s) of 100 Hz and 20 Hz, respectively.

Table 1. Demographic details of all the 15 subjects.

Gender (n)	Age (ME ± SD)	Weight(Kg) (ME ± SD)	Height(m) (ME ± SD)	BMI (Kg/m^2) (ME ± SD)
M (6)	29.6 ± 3.5	72.3 ± 15.9	1.7 ± 0.1	24.7 ± 5.1
F (9)	21.7 ± 0.4	55.6 ± 9.8	1.5 ± 0.1	22.7 ± 3.7

Notes: M: male, F: female, n: number of subjects, ME: mean, SD: standard deviation, BMI: body mass index.

feature,[27] and they are found within the normal range.

The Bland–Altman plot is employed for the validation purpose through assessing the agreement between the proposed and existing capnography devices measurements. As presented in Figs. 8–10, the upper and lower difference limits of CO_2, $EtCO_2$ and RR of the developed capnography device and standard capnography were 2.85 mmHg and −2.26 mmHg (14.03% and −11.41%), 3.63 mmHg and −3.33 mmHg (9.65% and −8.86%), and 2.31 bpm and −1.51 bpm (13.66% and −8.68%), respectively. In addition, the mean difference values, for all features, are close to zero which implies that the measurements of the developed device are reasonably consistent with those of the standard capnography device. Thus, the proposed device can be used as a reliable alternative to the current standard capnography in hospital settings and the home environment to help manage cardiopulmonary conditions.

5. Discussion

Herein, we report an inexpensive, light-weight, and portable capnograph for managing the cardiorespiratory status of human beings in clinical settings and the home environment by measuring a set of parameters (ICO_2, $EtCO_2$, and RR). In contrast to the traditional standard capnography (20 Hz), the proposed device acquires CO_2 signals with a higher sampling rate of 100 Hz and hence offers freedom for

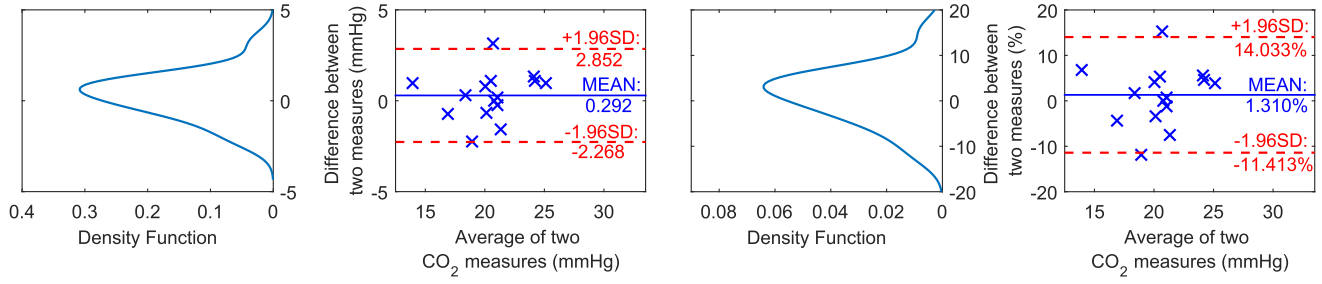

(a) (b)

Fig. 8. Bland–Altman plot of CO_2 measurements: (a) mean CO_2 vs. difference CO_2 (mmHg) and (b) mean CO_2 vs. difference CO_2 in percentage, along with corresponding density function plots; the dotted lines represent the upper and lower limits.

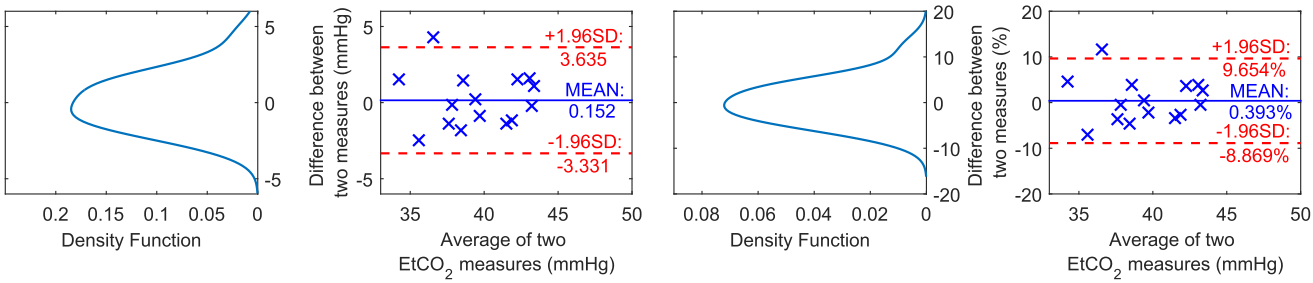

(a) (b)

Fig. 9. Bland–Altman plot of $EtCO_2$ measurements: (a) mean $EtCO_2$ vs. difference $EtCO_2$ (mmHg) and (b) mean $EtCO_2$ vs. difference $EtCO_2$ in percentage, along with corresponding density function plots; the dotted lines represent the upper and lower limits.

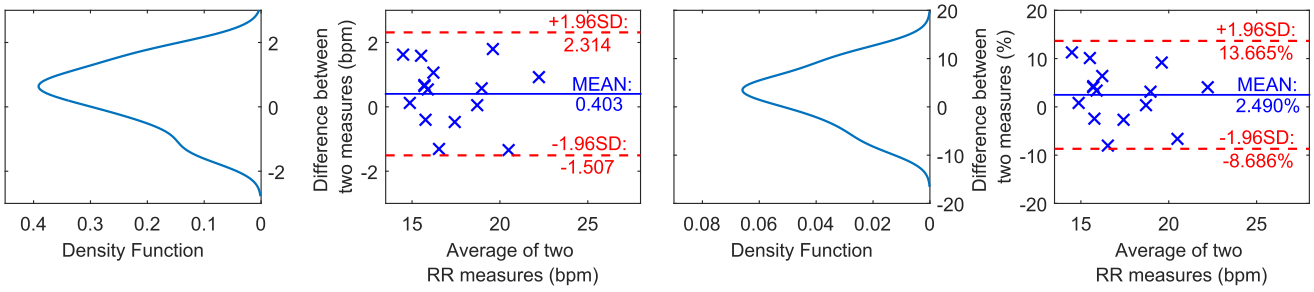

(a) (b)

Fig. 10. Bland–Altman plot of RR measurements: (a) mean RR vs. difference RR (bpm) and (b) mean RR vs. difference RR in percentage, along with corresponding density function plots; the dotted lines represent the upper and lower limits.

the further processing of CO_2 signals without resampling given that the CO_2 signal's of interest fall within 10 Hz.[22]

Additionally, the size and weight of the device reported here are less than those of the devices reported earlier by Santoso *et al.*[17,27] We had previously reported a real-time human respiration CO_2 measurement device and studied its behavior.[27] The brief description of the device's components and implemented algorithms for signal conditioning, features extraction and transmission may handicap the reproducibility of the results. Moreover, PCB fabrication was not performed.[27] This approach increased the size ($4.9 \times 5.1 \times 3.1$ inches) and weight (650 g) of the device. In addition, the storage capacity of the device is only 8 GB which restricts data-recording capacity. Furthermore, the power supply is external. Here, we present the final prototype with a reduced size ($4.5 \times 3.1 \times 1.8$ inches) and weight (450 g) and increased data storage capacity (16 GB). Additionally, two rechargeable batteries are utilized to drive the sensor, microcontroller, RTC and display. Accordingly, the current device can be transported anywhere without the need for an external power supply. The aforementioned modifications to the device will allow the management of respiratory disorders in and outside of hospital settings. Furthermore, the cost of the developed device is almost eight times less than that of existing devices on the market.[28] Hence, the current fabricated device is preferable over existing capnography devices. The performance of the device has been discussed in terms of accuracy.

The Bland–Altman plot provides two major important metrics, namely, bias and range of agreement, which are used to assess the precision of the proposed device. The mean difference between measurements represents the bias that reflects the average discrepancy between device measurements. The bias value ± 1.96 SD determines the range or limits of agreement within which approximately 95% of the differences between future measurements is expected to lie.

Figures 8–10 show that the differences between device measurements are positive for some samples and negative for other samples. This result implies that the measurements of the proposed device are sometimes greater and less than those of the existing device. In other words, no systematic error or bias exists in the measurements of the proposed device compared with those of the existing standard capnography device.

As can be also inferred from Figs. 8–10, the bias values between both devices are small and close to zero (i.e., no significant difference between the measurements recorded by both devices). Accordingly, in agreement with earlier studies reported by Critchley and Critchley[26] the difference between the measurements of the reference device lies within ±10%–20% relative to the bias. In addition, the density function plots show that the data points do not follow a certain trend because they are normally distributed, indicating that the differences among measurements are independent of their magnitude. Hence, the measurements of different parameter values (e.g., high measurement and low breathing rate) obtained by using the developed system are guaranteed. Furthermore, these results reveal that the differences between both device measurements are within the acceptable range.

6. Conclusion and Future Direction

We present an inexpensive, light-weight, and handheld prototype capnography device based on diverting technology for application in clinical settings and the home environment. Compared with those of a previously reported device, the size and weight of the developed device have reduced by 67% and 30%, respectively, facilitating the handling of the device. The device computes and displays the CO_2 signal, ICO_2, $EtCO_2$, and RR on a high-resolution display. In addition, this device provides smooth and sharp signals due to the integration of a noise reduction method that reduces the computational cost of the device. Furthermore, the proposed device has been tested and validated with 15 healthy subjects against a gold standard capnography device (Capnostream^{TM}20 Model CS08798) to determine its accuracy in measuring standard features. Findings revealed that the measured standard features, namely, CO_2, $EtCO_2$, and RR, are within the tolerance limit range (±10%–20%). Thus, the proposed device can be used in the hospital and home environment for the monitoring of cardiopulmonary conditions. In the future, the developed capnography device will be assessed with subjects suffering from cardiopulmonary disorders to verify its usability outside of the hospital setting.

Conflict of Interest

The authors report no conflict of interest. The authors alone are responsible for the content and writing of the paper.

Acknowledgments

This study was conducted as a part of the prototype research grant scheme, supported by Ministry of Higher Education, Government of Malaysia, under Grant no. Vote no. R.J130000.7851.4L919.

References

1. A. B. Sanders, K. B. Kern, C. W. Otto, M. M. Milander, G. A. Ewy, "End-tidal carbon dioxide monitoring during cardiopulmonary resuscitation: A prognostic indicator for survival," *JAMA* **262**(10), 1347–1351 (1989).
2. K. Z. Lukic, B. Urch, M. Fila, M. E. Faughnan, F. Silverman, "A novel application of capnography during controlled human exposure to air pollution," *Biomed. Eng. Online* **5**(1), 54 (2006).
3. P. A. Meaney, B. J. Bobrow, M. E. Mancini, J. Christenson, A. R. De Caen, F. Bhanji, B. S. Abella, M. E. Kleinman, D. P. Edelson, R. A. Berg *et al.*, "Cardiopulmonary resuscitation quality: Improving cardiac resuscitation outcomes both inside and outside the hospital: A consensus statement from the American heart association," *Circulation* **128**(4), 417–435 (2013).
4. S. Silvestri, G. A. Ralls, B. Krauss, J. Thundiyil, S. G. Rothrock, A. Senn, E. Carter, J. Falk, "The effectiveness of out-of-hospital use of continuous end-tidal carbon dioxide monitoring on the rate of unrecognized misplaced intubation within a regional emergency medical services system," *Ann. Emerg. Med.* **45**(5), 497–503 (2005).
5. O. K. Kurt, S. Alpar, T. Sipit, S. F. Guven, H. Erturk, M. K. Demirel, M. Korkmaz, M. Hayran, B. Kurt, "The diagnostic role of capnography in pulmonary embolism," *Amer. J. Emerg. Med.* **28**(4), 460–465 (2010).
6. K. Deitch, J. Miner, C. R. Chudnofsky, P. Dominici, D. Latta, "Does end tidal CO2 monitoring during

emergency department procedural sedation and analgesia with propofol decrease the incidence of hypoxic events? a randomized, controlled trial," *Ann. Emerg. Med.* **55**(3), 258–264 (2010).
7. C. A. Manifold, N. Davids, L. C. Villers, D. A. Wampler, "Capnography for the nonintubated patient in the emergency setting," *J. Emerg. Med.* **45**(4), 626–632 (2013).
8. J. M. Langlands, W. M. Wallace, "Small blood-samples from ear-lobe puncture a substitute for arterial puncture," *Lancet* **286**(7407), 315–317 (1965).
9. M. D. Davis, B. K. Walsh, S. E. Sittig, R. D. Restrepo, "AARC clinical practice guideline: Blood gas analysis and hemoximetry: 2013," *Respir. Care* **58**(10), 1694–1703 (2013).
10. A. Ak, C. O. Ogun, A. Bayir, S. A. Kayis, R. Koylu, "Prediction of arterial blood gas values from venous blood gas values in patients with acute exacerbation of chronic obstructive pulmonary disease," *Tohoku J. Exper. Med.* **210**(4), 285–290 (2006).
11. D. Flenley, "Arterial puncture," *Br. Med. J.* **281** (6233), 128 (1980).
12. P. Tosiri, N. Kanitsap, A. Kanitsap, "Approximate iatrogenic blood loss in medical intensive care patients and the causes of anemia," *J. Med. Assoc. Thai* **93**(suppl 7), S271–S276 (2010).
13. S. E. Huttmann, W. Windisch, J. H. Storre, "Techniques for the measurement and monitoring of carbon dioxide in the blood," *Ann. Am. Thorac. Soc.* **11**(4), 645–652 (2014).
14. S. Sudip, Capnography equipment market - global industry analysis, size, share, growth, trends and forecast 2014–2020, http://transparencymarketresearch.com, accessed 20 September 2017.
15. A. Y. Kumar, K. Bhavani-Shankar, H. S. Moseley, Y. Delph, "Inspiratory valve malfunction in a circle system: Pitfalls in capnography," *Can. J. Anaesth.* **39**(9), 997 (1992).
16. G. Schmalisch, "Current methodological and technical limitations of time and volumetric capnography in newborns," *Biomed. Eng. Online* **15**(1), 1–13 (2016).
17. D. Santoso, F. D. Setiaji, "Design and implementation of capnograph for laparoscopic surgery," *Int. J. Inf. Electron. Eng.* **3**(5), 523 (2013).
18. C. Bautista, B. Patel, M. Shah, L. Connie, B. Seifer, G. Facas, Portable capnography, http://portablecapnography.weebly.com/uploads/8/0/5/5/8055239/nebec_portable_capnography.pdf, accessed 5 October 2017.
19. S. Z. Binti Zaharudin, M. Kazemi, M. Malarvili, Designing a respiratory CO2 measurement device for home monitoring of asthma severity, *2014 IEEE Conf. Biomedical Engineering and Sciences (IECBES)*, IEEE, pp. 230–234 (2014).
20. S. A. Malik, O. P. Singh, A. Nurifhan, M. Malarvili, Portable respiratory CO2 monitoring device for early screening of asthma, *Proc. ACEC*, Rome, Italy, pp. 90–94 (2016).
21. K. Kuhn, E. Pignanelli, A. Schutze, "Versatile gas detection system based on combined NDIR transmission and photoacoustic absorption measurements," *IEEE Sensors J.* **13**(3), 934–940 (2012).
22. J. Yang, K. An, B. Wang, L. Wang, "New mainstream double-end carbon dioxide capnograph for human respiration," *J. Biomed. Opt.* **15**(6), 065007 (2010).
23. M. Kirkko-Jaakkola, J. Collin, J. Takala, "Bias prediction for MEMES gyroscopes," *IEEE Sensors J.* **12**(6), 2157–2163 (2012).
24. G. R. Arce, *Nonlinear Signal Processing: A Statistical Approach*, John Wiley & Sons (2005).
25. Q. Zhang, X. Zeng, W. Hu, D. Zhou, "A machine learning-empowered system for long-term motion-tolerant wearable monitoring of blood pressure and heart rate with ear-ecg/ppg," *IEEE Access* **5**, 10547–10561 (2017).
26. L. A. Critchley, J. A. Critchley, "A meta-analysis of studies using bias and precision statistics to compare cardiac output measurement techniques," *J. Clin. Monitor. Comput.* **15**(2), 85–91 (1999).
27. O. P. Singh, T. A. Howe, M. Malarvili, "Real-time human respiration carbon dioxide measurement device for cardiorespiratory assessment," *J. Breath Res.* **12**(2), 026003 (2018).
28. M. Richardson, K. Moulton, D. Rabb, S. Kindopp, T. Pishe, C. Yan, I. Akpinar, B. Tsoi, A. Chuck, Capnography for monitoring end-tidal CO2 in hospital and pre-hospital settings: A health technology assessment, *CADTH Health Technology Assessment*, 142 (2016).